Vailable online at www.sciencedirect.com

SciVerse ScienceDirect

Energy Procedia 27 (2012) 135 – 142

Energy Procedia

SiliconPV: April 03-05, 2012, Leuven, Belgium

Analysis of the Temperature Dependence of the Open-Circuit Voltage

P. Löper[a,c]*, D. Pysch[b], A. Richter[a], M. Hermle[a], S. Janz[a], M. Zacharias[c], S.W. Glunz[a]

[a]*Fraunhofer ISE, Heidenhofstr. 2, 79110 Freiburg, Germany*
[b]*Rena, 79110 Freiburg, Germany*
[c]*IMTEK, University of Freiburg, Georges-Koehler-Allee 103, 79110 Freiburg, Germany*

Abstract

The influence of temperature on the open-circuit voltage (V_{OC}) of crystalline silicon solar cells is analysed using different semiconductor temperature models with different levels of accuracy. The strongest influence besides the direct dependence of the intrinsic carrier concentration on temperature results from the temperature dependence of the band gap and the effective density of states, while the incomplete ionization plays a minor role for the implied voltage. However incomplete ionization can play an important role for the external voltage at temperatures below 50K due to imperfect selectivity of the emitter and back surface field. The observed saturation of V_{OC} towards low temperatures is caused by the effective density of states. The temperature dependence from 80 K to 300 K and the intensity dependence as a function of temperature and illumination density were measured on a silicon wafer solar cell resulting in a maximum voltage of 1012 mV at T=85.8K. The measured values could be well described by theory.

Keywords: Temperature-dependence; solar cells; intrinsic carrier concentration

1. Introduction

A detailed knowledge of the temperature dependence of the open-circuit voltage is important as for the design of concentrator as well as space solar cells, but also gives an interesting insight into various

* Corresponding author. Tel: +49-761-45885021; fax: +49-761-45889250
E-mail address: philipp.loeper@ise.fraunhofer.de

1876-6102
doi:10.1016/j.egypro.2012.07.041

physical mechanisms. The open-circuit voltage increases with decreasing temperature due to a reduction of the intrinsic carrier concentration. Recently, a value of V_{OC}=1104 mV at 4 K [1] was measured on an n-type Si solar cell. In this paper, four common temperature models with different levels of accuracy and the resulting functional dependence of V_{OC} are reviewed. It will be shown which physical value has the strongest influence on V_{OC}. The temperature dependence of a c-Si solar cell is measured and compared with the theoretical models.

2. Theory

2.1. Implied V_{OC} as a function of the temperature

The fundamental link between open-circuit voltage V_{OC} and temperature T is provided by the law of mass action, i.e. the requirement that the product of electron (n) and hole (p) concentrations is constant irrespective of temperature and illumination conditions:

$$n_i^2 = np \tag{1}$$

The electron concentration of electrons is given by the density of states $N(E)$ and the Fermi function $f(T,E,E_{F,n})$

$$n(T) = \int_{E_C}^{\infty} N(E) f(T, E, E_{F,n}) dE \tag{2}$$

where E_C is the conduction band edge. An analogous expression holds for holes. In thermal equilibrium $E_{F,n}$ is called the Fermi-level and the integral equals the dark carrier concentration, $n=n_0$. Under illumination, the parameter quasi-Fermi level $E_{F,n}$ describes the total carrier concentration $n=n_0+\Delta n$, Δn being the excess carrier density. In a non-degenerate semiconductor (E_C-E_F>>k_BT), the Fermi function can be approximated by the Boltzmann distribution. Integration of Eq. 2 results in

$$n = N_C \exp(-(E_C - E_{F,n}) / k_B T) \tag{3}$$

and analogously for holes. Eq. 1 then reads

$$p \cdot n = N_C N_V \exp(E_{F,n} - E_{F,p} - E_g) = n_i^2 \exp(e \cdot V_{OC,implied} / k_B T) \tag{4}$$

with e being the elementary charge, k_B being the Boltzmann constant and with $V_{OC,implied}$ being defined as ($E_{F,n}$-$E_{F,p}$)/e The same calculation in dark (charge carrier densities n_0, p_0 and $E_{F,n}$-$E_{F,p}$=0) provides the temperature dependence of the intrinsic carrier concentration. With this result, Eq. 4 can be solved for $V_{OC,Implied}$:

$$V_{OC,implied}(T) = \frac{k_B T}{e} \cdot \ln\left((p_0 + \Delta n) \cdot \Delta n / n_i^2\right) \tag{5}$$

In this paper, p-type material is considered and p_0 refers to the concentration of ionized acceptor impurities. In general, this value is the product of the ionization degree f_A and the total acceptor concentration N_A.

In order to identify the dominant effects in the temperature dependence of the open-circuit voltage, we compared four different models in this paper which are summarized in Table I. In the **simple model**, a full ionization of impurities, i.e. dopants, a constant band gap and constant densities of states are assumed and no temperature dependence of the charge carrier masses is taken into account. The **basic model** differs from the simple model in that it takes the temperature dependence of the density of states as N_C=N_C^{300K}·$T^{3/2}$ (accordingly for holes) into account. At low temperatures, not all impurities are ionized (freeze out) as taken into account in the **standard model**, which comprises the ionization degree f_A to describe the majority concentration up to 350°C: $p_0(T)$= $f_A(T,N_A,E_A)$·N_A. The ionization degree f_A is derived by considering the complete impurity population statistics [3]. The **advanced model** also

includes the temperature dependences of the band gap and the effective masses. For the band gap, we use the Varshni [2] formula with the parameterization as given in Sze [3]:

$$E_g(T) = E_g(0) - \alpha \cdot T^2/(T+\beta), \quad (6)$$

with $E_g(0)$= 1.17 eV, β=636K and α=4.73·10^{-4} eV/K. The temperature dependence of the effective masses m^* influences the effective density of states N_C (T, $m^*(T)$)=N_C^{300K} $m^*(T)^{3/2}T^{3/2}$ [4].

Table 1. The four different temperature models and their main assumptions at a glance.

	T-dep. density of states	Incomplete ionization	T-dep. band gap	T-dep. effective masses
Simple	No	No	No	No
Basic	$N_C = N_C^{300K} T^{3/2}$	No	No	No
Standard	$N_C = N_C^{300K} T^{3/2}$	$p_0(T) = f_A(T,N_A,E_A)\cdot N_A$	No	No
Advanced	See last column	$p_0(T) = f_A(T,N_A,E_A)\cdot N_A$	$E_g(T)=E_g(0)-\alpha T^2/(T+\beta)$	$N_C(T, m^*(T))=N_C^{300K}\cdot m^*(T)^{3/2}T^{3/2}$

Figure 1 depicts different cases: In the simple model, $V_{OC}(T)$ does not change its slope. The additional assumption of a temperature-dependent band gap results in a steeper $V_{OC}(T)$, but this curve still has a constant slope (not shown here). The next steps of complexity are the basic model with the $T^{3/2}$-temperature dependence of the effective masses, and the standard model, which also accounts for the majority carrier freeze out. It can be seen that freeze out is only a minor effect around 60 K. The standard model still differs considerably from the advanced model. However, if additionally the band gap temperature dependence is taken into account, both the basic and the standard model resemble well the advanced model (the case "Standard with $E_g(T)$" is omitted in Figure 1 for clarity). This means, that besides the direct dependence of n_i on T the next prominent effect on $V_{OC}(T)$ are the temperature dependences of the band gap and the density of states. The change in slope is due to the $T^{3/2}$–dependence of the effective density of states. Majority carrier freeze out and the temperature dependence of the effective masses play only a minor role.

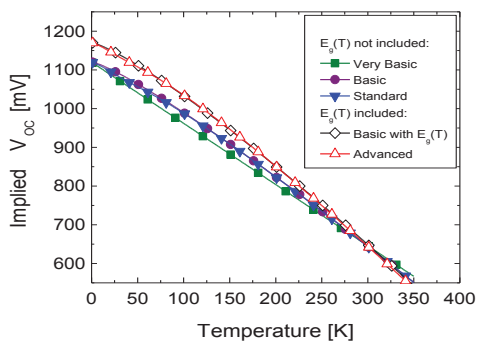

Fig. 1. Implied open-circuit voltage as a function of the temperature for five different scenarios to illustrate the major effects. All curves were calculated for p-type (Boron) Silicon with 1.5·10^{16} cm^{-3} base doping (1 Ωcm) and an excess carrier density of Δn=5·10^{14}cm^{-3}

2.2. Externally measured V_{OC}: Effects of the selective contacts (emitter and back surface field)

In the previous section, only the *implied* open-circuit voltage was considered. However, the *externally* measured voltage also depends on the selective contacts, i.e. emitter and back surface field (BSF), of the solar cell. According to [5], the external voltage can be described as a sum of the implied voltage and logarithmic terms accounting for the doping level and the excess carrier density in the emitter and BSF:

$$V_{OC,ext} = V_{OC,implied} - \frac{k_B T}{e} \cdot \ln\left((p_0 + \Delta n)/p_0\right) - \frac{k_B T}{e} \cdot \ln\left((n_0 + \Delta n)/n_0\right) \quad (7)$$

If the emitter or BSF are in high injection, i.e. the excess carrier density in the order of the doping concentration, the external voltage is lower than the implied voltage. The condition of "high injection" depends on the temperature because the freeze out of charge carriers changes the ratio $N_A/\Delta n$. Therefore, the functional dependence of $V_{OC,ext}(T)$ has to be considered when the temperature dependence of *externally* measure voltages is evaluated.

The temperature dependence of the external voltage is modeled straight forward according to Eq. 5 by taking into account carrier freeze out, as discussed above for the standard and advanced temperature model (see also Table I). Figure 2 shows a plot of $V_{OC,ext}(T)$ for excess carrier densities of 10^{14} cm^{-3} and 10^{16} cm^{-3} along with $V_{OC,implied}(T)$, all calculated with the advanced temperature model. It can be seen that the external voltage drops below a certain transition temperature. At the transition temperature, the ionization degree f_A gets so low that the excess carrier density Δn exceeds the doping density $f_A \cdot N_A$. In other words, the doped regions of the device change from being operated in low injection to high injection. Because higher doped material has a higher freeze out temperature, the voltage drop also occurs at higher temperatures, see Fig. 2, (right). Fig. 2 (left) demonstrates that for excess carrier densities in the order of $<10^{16}$ cm^{-3} and for $T>50$K the voltage drop due to the highly doped regions can be neglected. Because in this study only temperatures >77K are considered, we approximate $V_{OC,ext}(T) \approx V_{OC,implied}(T)$.

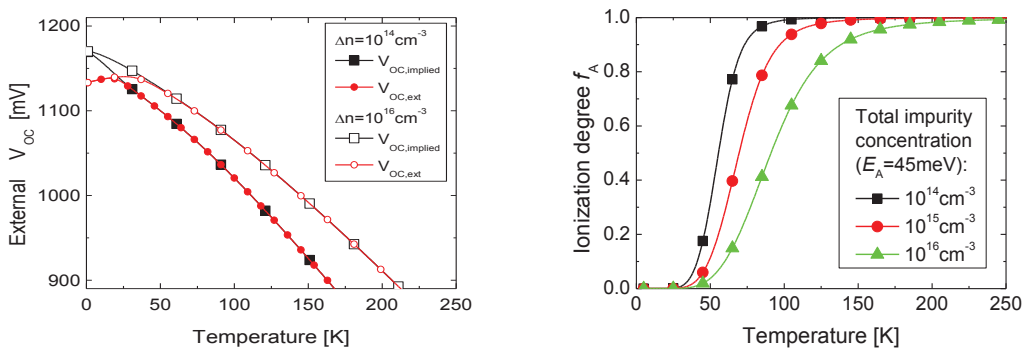

Fig. 2. (Left) Temperature dependence of the external and implied open-circuit voltage as calculated from equations (5) and (7), respectively. The advanced temperature model was applied and freeze out in the emitter and BSF was included. The calculation was done for a p-type (Boron) 1Ωcm wafer with $1.5 \cdot 10^{16}$ cm^{-3} base doping with a boron BSF ($4 \cdot 10^{19}$ cm^{-3}) and a phosphorus emitter ($1.5 \cdot 10^{20}$ cm^{-3}). The activation energies for boron and phosphorus were set to 30 meV and 45meV, respectively.
(Right) Ionization degree of boron (activation energy 45 meV) as a function of temperature

3. Experimental

In this paper, a back-contact back-junction solar cell based on a 1 Ωcm FZ p-type (boron) wafer was studied. The selective contacts were formed by phosphorus and boron diffusion and a phosphorus floating emitter was implemented for front surface passivation. Details on the solar cell can be found in [6]. The measurement was done in a nitrogen-cooled cryostat with an UV transmittive optical window. During the temperature-dependent measurements, the cell temperature was measured with a PT100 next to the cell in direct contact to the copper plate onto which the cell was mounted. IV-curves were recorded using a sun simulator as illumination source. For the temperature and intensity dependent measurements, a Xe lamp was used. In all cases, the illumination density was monitored with a reference solar cell.

4. Results and Discussion

4.1. Temperature dependence

The solar cell was measured under different conditions: The full IV-curve, the temperature dependence of V_{OC}, and the intensity dependence of V_{OC} at different temperatures. The full IV-curve, measured at 300K and 79K at an irradiation intensity of 1.1 suns is shown in Fig. 3. At 79K, V_{OC}=941 mV was measured, compared to a value of 606 mV at 300K. The current drops from 16.4 mA/cm^2 at 300K to 5.7 mA/cm^2 at 79K.

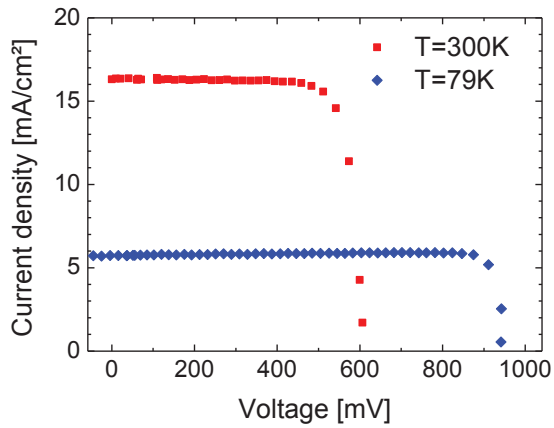

Fig. 3. IV-curves under illumination of 1.1 suns at 300K and 79K

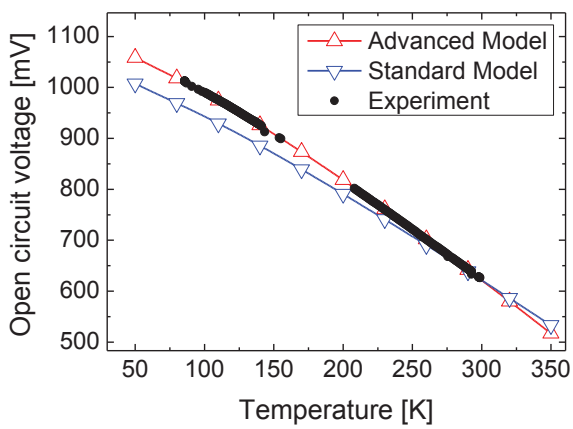

Fig. 4. Measured V_{OC} (black dots) from 80 K to 300 K and theoretical V_{OC} according to the standard and the advanced model. A change of the slope can clearly be observed. The theoretical curves were calculated with $1.5 \cdot 10^{16}$ cm^{-3} base doping, an irradiation intensity of 2.6 Suns and an offset of -52 mV to resemble the measured value at room temperature

The temperature dependence $V_{OC}(T)$ is shown in Figure 4 (black dots) together with theoretical curves (red and blue lines) according to the standard and the advanced model. The highest values for V_{OC} reach a value of 1012 mV at 85.8 K. Obviously, the voltage of a real solar cell with non-ideal recombination is

lower than the theoretical limit. For a given short-circuit current, the open-circuit voltage is determined by J_0 under the assumption of the one-diode model with an ideality factor of 1:

$$V_{OC}(T) = \frac{k_B T}{e} \cdot \ln\left(J_{SC} / J_0\right) + 1\Big). \tag{8}$$

In this equation, a higher J_0 (lower voltage) translates to a smaller argument of the logarithm which in the approximation of $J_{SC}/J_0+1 \approx J_{SC}/J_0$ is equal to adding a constant offset. Therefore, an offset $V_{OC,}$ Theory300 K) was introduced to Eq. 5 which was treated as a fit parameter to adjust the theoretical value to the experimental V_{OC} at 300K. In this experiment, Δn was not determined independently and thus treated as a second free parameter in the fit of Eq. 5 to the experimental data. It has to be noted that after the temperature-dependent measurement shown in Fig. 4, additional measurements were done that led to a degradation of the solar cell. Afterwards, the IV curves shown in Fig. 3 were recorded. Because the data in Fig. 3 are not comparable to the data in Fig. 4, the excess carrier density could not be determined, as mentioned before. Good agreement is achieved with an offset of -0.52 mV and an illumination intensity of 2.6 suns, as shown in Fig. 4. The base doping N_A was set to $1.5 \cdot 10^{16}$ cm^{-3}, corresponding to the 1 Ωcm base material (boron) the cell was made of. It is also noted that within a variation of 10^{14} cm$^{-3} \leq \Delta n \leq 10^{15}$ cm^{-3} and $0 \leq V_{OC}(300\ \mathrm{K}) \leq 100$ mV, no agreement between the standard model and the experiment (data shown in Fig. 4) could be found. This clearly demonstrates the importance to take the full advanced model (especially including the temperature dependence of the band gap and the effective density of states), into account.

4.2. Intensity dependence

The open-circuit voltage rises logarithmically in first order approximation with the illumination intensity as is evident from Eq. 5. However, it is to be expected that this increase saturates before the quasi-Fermi levels reach the bands. For a more detailed understanding of the temperature behaviour, the intensity dependence of the open-circuit voltage was measured and compared to the theory. Note, that within the theoretical framework used here we assumed that the excess carrier concentration is proportional to the generation rate $\Delta n = G \cdot \tau$ and not temperature dependent. In general, this is not true: Defect spectroscopy [4] exploits the temperature and the intensity dependence of the charge carrier lifetime $\tau(\Delta n, T)$ to extract recombination parameters of defects in the Si bulk.

Intensity-dependent measurements were performed at different set temperatures of the cryostat. However, the cell temperature changes with the irradiation intensity also for the same set temperature of the cryostat. This results in a broad scattering of the data. The entire set of data is plotted in Figure 5 (left). In order to account for the real cell temperature, the voltages were corrected in first order using the partial derivative of the theoretical voltage:

$$V_{OC}^{corrected}(T, I) \approx V_{OC}^{\exp}(T_{Cell}, I) + (T - T_{Cell}) \frac{\partial V_{OC}^{Theory}(T_{Cell}, I)}{\partial T} \tag{9}$$

T_{Cell} is the temperature measured with a PT100 on the copper plate the cell was mounted to and directly next to it. The correction was done for 120K. Fig. 5 shows the corrected values along with the theory. The corrected values are in well agreement with each other. Interestingly, the difference between the theoretical curve and the corrected experimental data is approximately constant and similar to the voltage offset in Fig. 4. This result confirms that the open-circuit voltage is well described by the model presented in this paper, and that the simplification of neglecting changes in Δn as the temperature changes is justified.

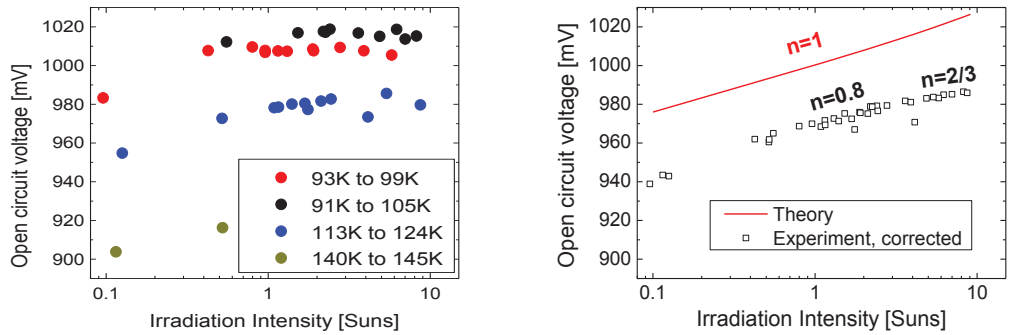

Fig. 5. (Left) Intensity dependent measurement of the open-circuit voltage for four temperature ranges. For low temperatures, a saturation of the voltage can be observed. Because the solar cell temperature is strongly influenced by the actual irradiation intensity, the data are scattered. After correction for the cell temperature deviation from 120K, all data points are in very well in accordance (see text). The theoretical $V_{OC}(I)$, calculated with the advanced model at 120K is shown for comparison (red line). The difference to the experimental data arises because no voltage offset like for the fit shown in Fig. 4 was accounted for.

5. Conclusion and Outlook

In this paper, the dependence of the open-circuit voltage on the solar cell temperature and irradiation intensity was investigated. Several temperature models were compared theoretically. Beside the direct temperature dependence of the intrinsic carrier density, the most prominent effect influencing V_{OC} stems from the band gap temperature dependence. Towards lower temperatures, the $V_{OC}(T)$ curve changes its slope due to the $T^{3/2}$-temperature dependence of the effective densities of states. Incomplete ionization ("freeze out") and the effective masses only have a minor impact on the implied voltage. However, freeze out within the selective contacts is responsible for a drop of the external voltage towards low temperatures (T<50K). For temperatures >50K and doping concentrations $<10^{16}$cm^{-3} (Boron), the external voltage is not influenced by temperature effects of the emitter or back surface field and may be used as an approximate to the implied V_{OC}. The theoretical framework presented in this paper allows an accurate modelling of the open-circuit voltage as a function of the temperature and illumination intensity. The combination of the intensity and temperature dependence yields a description for quasi steady state (QSS)-$V_{OC}(T)$ data. A series of QSS-V_{OC} [7] measurements at different temperatures provides the pseudo-IV curve and the lifetime $\tau(T)$ at the temperatures considered. This enables a defect characterization on device level, and thus of e.g. thin film materials to which QSS photoconductance or QSS photoluminescence cannot be applied.

Acknowledgements

The authors are thankful to Anke Witzky and Tim Niewelt for help with the cryogenic systems. P. L. gratefully acknowledges the scholarship support of the Reiner Lemoine Stiftung and the ideational support of the Heinrich Böll Stiftung.

References

[1] G. Willeke and R. Hoheisel, *private communication,* 2011.

[2] Y. P. Varshni, "Temperature dependence of the energy gap in semiconductors," *Physica,* vol. 34, pp. 149-54, 1967.

[3] S. M. Sze, *Semiconductor devices, Physics and Technology.* , 2 ed. Hoboken, New Jersey, USA: John Wiley & Sons Inc. , 2001.

[4] S. Rein, T. Rehrl, W. Warta, and S. W. Glunz, "Lifetime spectroscopy for defect characterization: Systematic analysis of the possibilities and restrictions", *Journal of Applied Physics*. vol. 91, pp. 2059-2070 (2002).

[5] D. Pysch*, et al.*, "Analysis and optimization approach for the doped amorphous layers of silicon heterojunction solar cells," *Journal of Applied Physics,* vol. 110, p. 094516, 2011. and P. Würfel, "Physics of solar cells", Weinheim: Wiley-VCH, 2005.

[6] A. Mohr*, et al.*, "Silicon concentrator cells with compound parabolic concentrators," in *Proceedings of the 19th European Photovoltaic Solar Energy Conference*, Paris, France, 2004, pp. 2537-40. and A. Mohr*, et al.*, " Influence of grid finger and busbar structure on the performance of rear-line-contacted silicon concentrator cells," in *Proceedings of the 19th European Photovoltaic Solar Energy Conference*, Paris, France, 2004, pp. 721-4.

[7] M. J. Kerr*, et al.*, "Generalized analysis of quasi-steady-state and transient decay open circuit voltage measurements," *Journal of Applied Physics,* vol. 91, pp. 399-404, 2002.